High-resolution probing of cellular force transmission

Daisuke Mizuno[1], Rommel Bacabac[2], Catherine Tardin[3], David Head[4], Christoph F. Schmidt[5]
[1] *Organization for the Promotion of Advanced Research, Kyushu Univ., 812-8581, Fukuoka, Japan*
[2] *Department of Oral Cell Biology, ACTA-Vrije Universiteit, 1081 BT Amsterdam, The Netherlands*
[3] *IPBS/CNRS, 205 Route de Narbonne, 31062 Toulouse Cedex, France*
[4] *Institute of Industrial Science, University of Tokyo, Meguro-ku, Tokyo 153-8505, Japan and*
[5] *III. Physikalisches Institut, Georg-August-Universität, 37077 Göttingen, Germany*
(Dated: November 15, 2008)

Cells actively probe mechanical properties of their environment by exerting internally generated forces. The response they encounter profoundly affects their behavior. Here we measure in a simple geometry the forces a cell exerts suspended by two optical traps. Our assay quantifies both the overall force and the fraction of that force transmitted to the environment. Mimicking environments of varying stiffness by adjusting the strength of the traps, we found that the force transmission is highly dependent on external compliance. This suggests a calibration mechanism for cellular mechanosensing.

PACS numbers: 83.80.Lz, 83.85.Ei, 87.16.dj, 87.16.dm, 87.16.Xa, 87.17.Rt

Cells, be they single cell organisms or part of a tissue, constantly communicate with their environment. Apart from exchanging chemical signals, cells perform mechanosensing, *i.e.* they both sense external forces and actively probe the mechanical properties of the environment they are embedded in [1, 2]. Signaling cascades initiated by mechanosensing influence cell growth, development and fate. Just like an engineer would do, cells explore external material properties by imposing a force and measuring the response. Cells generate forces by contracting their "inner muscles", *i.e.* the *cytoskeleton*, composed largely of actin networks and bundles (stress fibers), actuated by myosin motor proteins [3]. The cytoskeleton is coupled to the external environment *via* specialized adhesion contacts, the focal adhesions [4, 5]. Cellular stress sensors are believed to be localized at the focal adhesions [6, 7].

The physical and molecular details of stress sensing remain largely unknown. It has been difficult to quantify stresses and forces in cells due to their complex shapes and internal structures. The fraction of the internally generated force that is transmitted to the environment will furthermore depend on the mechanical properties of both the cell and the environment, and on the exact geometry of cell adhesion. Here we present a new experimental approach that allows us to measure simultaneously the cell's viscoelastic response, the overall force the cell generates, and the fraction of the force that is transmitted to the environment. In the simplified geometry of a close-to-spherical cell shape, suspended between two optically trapped colloidal beads, we demonstrate how the transmitted force directly scales with the external stiffness. This result suggests a mechanism by which cells can calibrate their own active mechanosensing machinery.

The approach we use is a variation of optical-trap based microrheology (MR) which can be done actively (AMR) [8–11] or passively by tracking fluctuations (PMR) [12–14]. Both AMR and PMR can be performed with single probe beads [12, 13] or by evaluating correlated motions of pairs of probes [14–16]. We have carried out 2-particle AMR and PMR simultaneously on osteocyte-like MLO-Y4 cells [17]. This was necessary in order to be able to dissect the non-equilibrium fluctuations generated by the cellular traction forces from the thermal fluctuations. The latter are intimately connected to the cell's response characteristics *via* the fluctuation-dissipation theorem. We measured the motion of the optically trapped probe particles using laser interferometry and quadrant photodiodes with a spatial resolution better than 0.1 nm [18, 19]. To create two optical traps, we focused two laser beams (λ = 1064 nm, Nd:YVO_4, Compass, Coherent) with orthogonal polarizations in a custom-built microscope to diffraction-limited spots [15]. For AMR, one particle was oscillated using an acousto-optical deflector [10]. The output signal from the photodiode that detects the position of the other particle was measured with a lock-in amplifier. Position measurements were done relative to the centers of the optical traps. Through the independently determined trap stiffness, displacement translates directly to a force on a bead. For PMR, the oscillation of the driving laser was turned off, and the spontaneous fluctuations in the positions of both particles were recorded. Displacements and trap stiffnesses were calibrated by recording fluctuations of beads from the same batch in water [10, 13, 20]. Cells were cultured and prepared for experiments as described in ref. [21]. Polystyrene beads (4 μm diameter) coated with fibronectin, which promotes integrin-mediated adhesion, were attached to opposite sides of a cell and held in suspension by the optical traps [21]. Cells thus remained roughly spherical (Fig. 1a). Experiments were carried out in a CO_2-free culture medium at 37° C. Lipid vesicles coated with F-actin were used as controls, following the procedure described in ref. [22].

For 2-particle AMR, the response functions A_{ij} =

$A'_{ij} + iA''_{ij}$ defined by $A_{ij} \equiv u_j/d_i$ was obtained by measuring the displacement u_j of particle j, caused by the driving force d_i on particle i, in the direction parallel to the line connecting the two particles. For 2-particle PMR, the Fourier transform of the cross-correlation function of the spontaneous bead fluctuations $\langle u_i(\omega)\, u_j^*(\omega)\rangle \equiv \int \langle u_i(t)\, u_j(0)\rangle \exp(i\omega t)dt$ was calculated. In equilibrium, the fluctuation-dissipation theorem relates this function $\langle u_i u_j^*\rangle$ to the imaginary part of the complex response function A''_{ij} by

$$P_{th}(\omega) = 2k_BTA''_{ij}/\omega \qquad (1)$$

The real part A'_{ij} is estimated through a Kramers-Kronig integral: $A'_{ij}(\omega) = \frac{2}{\pi}P\int_0^\infty \frac{\zeta A''_{ij}(\zeta)}{\zeta^2-\omega^2}d\zeta$, where P denotes a principal-value integral. In non-equilibrium systems such as living cells, however, both thermal and actively-generated forces act on the probes. Here it is critical to combine AMR and PMR in the same experiment so that we can separate the active from the thermal fluctuations [10]. AMR gives the material response function A_{ij}, from which we can estimate the thermal part of the fluctuations $2k_BTA''_{ij}/\omega$ *via* the FDT. Provided that thermal and non-thermal fluctuations are uncorrelated, the non-thermal fluctuation spectrum $P_{act}(\omega)$ can then be determined as the difference between the total spectrum measured by PMR and the thermal spectrum estimated by AMR:

$$P_{act}(\omega) = \langle u_i u_j^*\rangle - 2k_BTA''_{ij}/\omega \qquad (2)$$

This expression quantifies the extent of mechanical non-equilibrium in the system. The physical origin of $P_{act}(\omega)$ depends on the system under investigation [23]. Here we will proceed to calculate from $P_{act}(\omega)$ the frequency dependence of the active traction forces that the cells exert on their environment, which is in this case represented by the optically trapped beads.

Fig. 1b shows the fluctuations in the measured forces $ku_1(t)$ and $ku_2(t)$ for each probe as a function of time, where k is the trap stiffness which was adjusted to be equal in the two traps. The forces felt by the two particles appear largely balanced, *i.e.* they add to zero, which suggests that intracellularly generated forces are predominant in driving the slow fluctuations. For comparison, the same experiment was carried out with an actin-coated vesicle in thermodynamic equilibrium (Figs. 1c and d), where no such large and slow fluctuations were seen. The response function of an MLO-Y4 cell is shown in Fig. 2a, where open circles give the normalized fluctuation cross correlation $\omega\langle u_1u_2^*\rangle/2k_BT$ measured by PMR, and closed circles give the response function A_{12} measured directly by AMR. At frequencies higher than 10 Hz, AMR and PMR show good agreement, as if the system was in equilibrium. At lower frequencies, in contrast, the PMR result shows a large negative correlation while A''_{12} measured by AMR is negligibly small and A'_{12} is

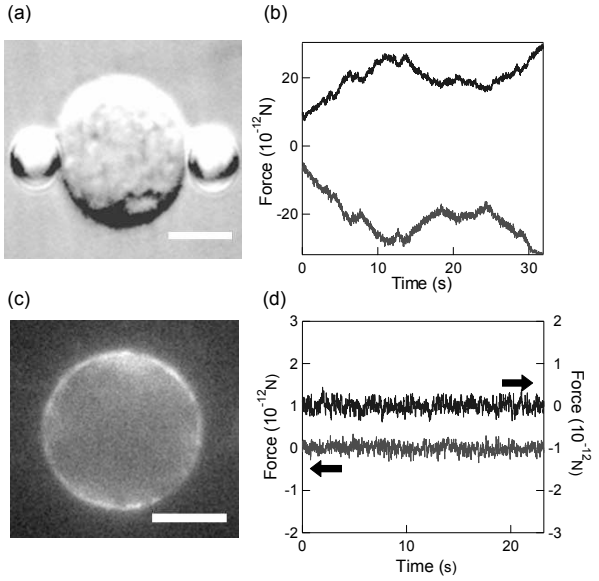

FIG. 1: (a) Differential interference contrast microscopy (DIC) image of a MLO-Y4 osteocyte-like cell suspended in culture medium by two optically trapped fibronectin-coated beads (diameter $2R = 4$ μm). The beads are attached to opposing sides of the cell. Scale bar: 5 μm (b) Fluctuations of the force exerted by the cell on both probe beads ($k = 5.0 \times 10^{-5}$ N/m). Forces generated by the cell result in anti-correlated displacements in the traps. (c) Fluorescence microscopy image of a lipid vesicle coated with rhodamine-phalloidin stabilized and biotinylated actin. Scale bar: 5 μm. (d) Thermal force fluctuations seen by the probe beads. Streptavidin coated beads were attached to the vesicles via the biotinylated actin.

roughly constant. At frequencies lower than 10 Hz, the mechanical response of the cell is thus quasi-static, but the observed violation of the FDT shows that the system is out of equilibrium. Fluctuations here are dominated by the non-equilibrium cellular forces.

Having isolated the non-equilibrium fluctuations, we now analyze their spectral characteristics and speculate about the underlying cellular processes creating these fluctuations. Fig. 3a shows that the power spectra of the active traction force fluctuations transmitted to the probe particles, $-k^2\langle u_1u_2^*\rangle$, approximately follow a scaling law $-k^2\langle u_1u_2^*\rangle \sim \omega^{-2}$ with an amplitude that depends on the trap stiffness k. The spectral density at 0.19 Hz is plotted versus k in Fig. 3b and shows a monotonic increase with k for small trap stiffnesses, appearing to asymptotically level off at high trap stiffnesses. This result, at first glance, appears to suggest that the cells generate more force when pulling against a stiffer trap. The simpler explanation of the observed force spectra is, however, that the internally generated forces both deform the cell itself and displace the beads in the traps, all of which can be modeled as coupled harmonic springs (Fig. 4). How the elastic energy is divided up between

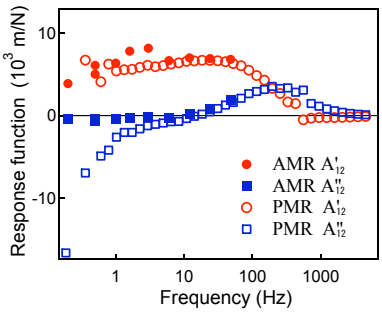

FIG. 2: A_{12} measured with AMR (filled symbols) compared to the normalized fluctuation power spectral density measured with PMR (open symbols). Circles and squares show real and imaginary parts, respectively. At frequencies lower than 10 Hz, a violation of the FDT was observed due to the traction forces generated by the cell.

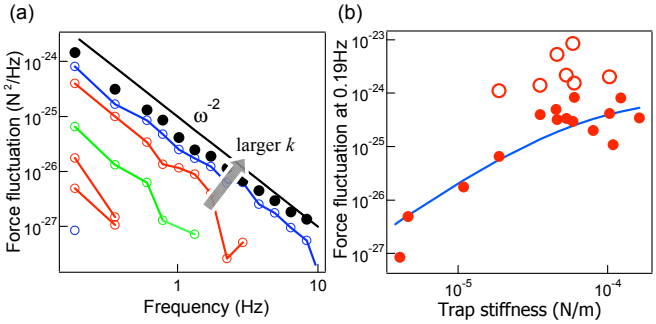

FIG. 3: (a) Trap-stiffness dependence of the (attenuated) force fluctuations detected by the beads $-k^2\langle u_1 u_2^*\rangle$. The power spectral density of the total fluctuating force $\langle FF^*\rangle$ (filled circles) follows an ω^{-2} power law. (b) Trap stiffness dependence of the force fluctuation $-k^2\langle u_1 u_2^*\rangle$ at 0.19 Hz (filled circles). The solid line is the fit of Eq. (2) to the data. The total traction force generated by the cell (open circles) does not depend on the strength of optical trapping.

the cell and the traps depends on the relative stiffnesses. When the optical trap is weak, internally generated forces mainly deform the cell, but when the traps are stiff, forces are efficiently transmitted to the probe particles without significantly deforming the cell. In this way, the optical traps and the beads suspending the cell assume the role of an elastic environment that would usually be provided by an extracellular matrix or neighboring cells, but which can now be conveniently controlled by the trapping laser power.

To quantify these ideas, we model the cell and the optical traps as coupled springs (Fig. 4). Here, k_{12} denotes the effective elastic constant of the cell. When balanced forces F and $-F$ are generated, the displacements of the probe particles are $u_1 = -u_2 = -F/(k+2k_{12})$, which gives

$$-k^2\langle u_1 u_2^*\rangle = \frac{k^2}{(k+2k_{12})^2}\langle FF^*\rangle \qquad (3)$$

We obtained both cell stiffness (16 measurements with 5 different cells) $k_{12} = 3.8 \pm 2.1 \times 10^{-5}$(N/m) and total cellular force generation $\langle FF^*\rangle$ (0.19 Hz) $= 1.4 \pm 1.0 \times 10^{-24}$(N^2/Hz) by fitting Eq. (2) to the data. The resulting value for k_{12} is consistent with the value directly obtained from AMR (force-distance curve) [21].

In order to extend this model to a general frequency-dependent response, we consider the Langevin equation for the two probe particles,

$$\int_{-\infty}^{t}\{\xi_{11}(t-t')\dot{u}_1(t') + \xi_{12}(t-t')\dot{u}_2(t')\}\,dt' = -ku_1 + K_1 + F_1 \qquad (4)$$

and similarly for switched indices. Here, K_i is the thermally fluctuating force acting on particle i, and $F_2 = -F_1 = F$ is the total traction force between probes. It is important to properly take into account the fact that the probes feel both, the viscoelastic response of the cell, and the confinement potentials ot the traps. The drag coefficient tensor ξ_{ij} describes only the cell response. The random thermal force, however, is related via the FDT to the total drag coefficient tensor of the system, including the trap effects, $\gamma_{ij}(= 1/i\omega A_{ij})$ by $\langle K_i K_j^*\rangle = 2k_B T\gamma_{ij}$. The cross-power spectrum is calculated via the Fourier transform of Eq. (4) as

$$\langle u_i u_j^*\rangle = -\langle FF^*\rangle (A_{11} - A_{12})(A_{22}^* - A_{12}^*) \qquad (5)$$

Open circles in Fig. 3b show the total traction force obtained from this model which is not measurably influenced by trap stiffness. The force transmitted to the probes, on the other hand, does vary with trap stiffness and only at large k converges towards the total traction force. Note that comparing AMR and PMR in Eq. (4) lets us obtain the total traction force without making the assumptions used in Eq. (3). Eq. (3) neglects thermal forces and assumes a quasi-static mechanical response, which was justified here merely because AMR $A_{12}'' \approx 0$ at low frequencies (Fig. 2).

It remains to link the observed force fluctuations between the two beads to microscopic molecular events in the cell. We here provide a simple scaling discussion. The generators of cellular force are motor proteins acting within the cytoskeleton. In many cell types, bipolar aggregates of cytoplasmic myosins bridge F-actin filaments or bundles and, under ATP hydrolysis, generate contractile forces [24]. Since one can often neglect external forces (such as gravitational, or electrostatic forces) reaching into the cell, each such elementary force-generating unit can be modeled as an internally-balanced force dipole [25]. We now derive an approximate expression for the displacement field u at a distance r from a single dipole in the low-frequency quasi-static limit where the elastic response of the cell dominates. Suppose the dipole consists of forces $\pm f$ separated by a distance ε.

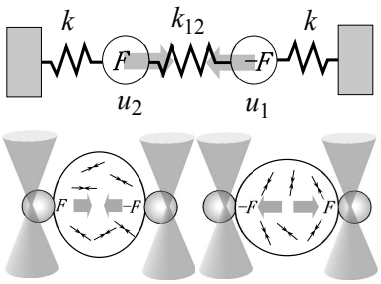

FIG. 4: Simple model of the mechanical components in our experimental configuration. k_{12} and k denote the stiffnesses of the cell and the optical traps, respectively, u_1, u_2 are the displacements of each particle. F denotes the total traction force as a sum of local forces as sketched in the lower panel.

To leading order in ε, and for a linear elastic response, u must be proportional to $\varepsilon f/\mu$ with μ the shear modulus [26]. For the probe particles attached to opposing cell boundaries, the distance to the force generators is of order $r \sim R$. The only possible scaling form for u driven by a single intracellular dipole is then $u \sim \varepsilon f/\mu R^2$. The direction of the total force dipole is dependent on the average orientation of local force generators as shown in Fig. 4 (lower panel). Assuming, for the sake of simplicity, that the activities and directions of local dipoles are uncorrelated, their collective activity driven by N dipoles in the cell over a volume $\sim R^3$ then gives a product $u^2 \sim N(\varepsilon f/\mu R^2)^2$. Inserting reasonable values for a cell ($\varepsilon \approx \mu$m, $f \approx$ pN, $\mu \approx 100$ Pa [21], $N \approx 1000$, and $2R \approx 10$ μm) results in $u^2 \sim 10^{-16}$ m^2. This estimate correponds to the mean square displacement explored by the probe particles within ≈ 1 s (Fig. 1b). Larger fluctuations on longer time scales are likely driven by the correlated activity of force dipoles which scales as $u^2 \sim N^2(\varepsilon f/\mu R^2)^2 \sim 10^{-13}$ m^2, still consistent to our data (Fig. 1b).

The approximate $\langle FF^* \rangle \sim \omega^{-2}$ frequency dependence which we have seen here in the extra-cellularly detected forces shown in Fig. 2b has also been widely seen with probes embedded in cells [16, 27], suggesting a common origin. The same frequency dependence has furthermore been observed in non-equilibrium model cytoskeletal networks activated by myosins [11]. The origin of this scaling behavior in the latter case appeared to be the occurrence of sudden force release events [11, 28]. Here, in our cell experiments, however, such release events were not evident, leaving the case somewhat open for further inquiry. Note that it is easy to confuse the non-equilibrium fluctuations in viscoelastic cells with diffusion in a purely viscous environment which produces the same power law.

Cellular forces have been examined using AFM or (micro-patterned) elastic substrates [7, 31]. These techniques detect merely the force transmitted to the probes, which depends on substrate response even if total cellular force generation remains the same, as we have shown. This fact has been largely neglected. The uniqueness of our approach is the ability to measure "total" cellular force as well as transmitted force.

Cells exhibit threshold responses that point to a mechanism that somehow performs a comparison between internal and external stiffness. For fibroblasts it was found [29] that stress fibers (F-actin/myosin bundles) are created only when the substrate elasticity is greater than 3 kPa, which is comparable to the cell elasticity. Differentiating mesenchymal stem cells can even adapt their own rigidity to their environment [30]. The comparison between inside and outside elastic response could be very directly performed by a force sensor located at the cell membrane, e.g. at focal adhesion complexes [4, 5], because, as we have shown here, the intracellularly generated force is only efficiently transmitted to the extracellular matrix when the stiffness of the surrounding matrix is larger than that of the cell itself.

Since it is becoming more and more evident that mechanosensing is a crucial component of cell-cell and cell-tissue communication, understanding the physical mechanisms at the basis of these cellular sensory capabilities will be relevant for both understanding cell development and differentiation and for applications in tissue engineering.

Acknowledgments: We thank A. Lau, F. MacKintosh for helpful discussions and J. Klein-Nulend and T. Smit for supplying cell cultures. This work was supported by the Sonderforschungsbereich SFB755 of the German Research Foundation (DFG) and by the DFG Center for the Molecular Physiology of the Brain (CMPB). D.M. was further supported by KAKENHI, a Program for the Improvement of the Research Environment for Young Researchers from SCF (Japan).

[1] V. Vogel and M. Sheetz, Nat. Rev. Mol. Cell Biol. **7**, 265 (2006).
[2] D. E. Discher, P. Janmey, and Y. L. Wang, Science **310**, 1139 (2005).
[3] M. R. K. Mofrad and R. D. Kamm, *Cytoskeletal mechanics : Models and measurements* (Cambridge University Press, Cambridge, 2006).
[4] J. Y. Shyy and S. Chien, Circ. Res. **91**, 769 (2002).
[5] H. B. Wang, M. Dembo, S. K. Hanks *et al.*, Proc. Natl. Acad. Sci. USA **98**, 11295 (2001).
[6] B. Geiger, A. Bershadsky, R. Pankov *et al.*, Nat. Rev. Mol. Cell Biol. **2**, 793 (2001).
[7] N. Q. Balaban, U. S. Schwarz, D. Riveline *et al.*, Nat. Cell Biol. **3**, 466 (2001).
[8] L. A. Hough and H. D. Ou-Yang, Phys. Rev. E **65**, 021906 (2002).
[9] D. Mizuno, Y. Kimura, and R. Hayakawa, Phys. Rev. Lett. **87**, 088104 (2001).
[10] D. Mizuno, D. A. Head, F. C. MacKintosh, and C. F. Schmidt, Macromolecules **41**, 7194 (2008).

[11] D. Mizuno, C. Tardin, C. F. Schmidt *et al.*, Science **315**, 370 (2007).
[12] T. G. Mason and D. A. Weitz, Phys. Rev. Lett. **74**, 1250 (1995).
[13] B. Schnurr, F. Gittes, F. C. MacKintosh, and C. F. Schmidt, Macromolecules **30**, 7781 (1997).
[14] F. Gittes, B. Schnurr, P. D. Olmsted, F. C. MacKintosh, and C. F. Schmidt, Phys. Rev. Lett. **79**, 3286 (1997).
[15] M. Buchanan, M. Atakhorrami, J. F. Palierne *et al.*, Macromolecules **38**, 8840 (2005).
[16] A. W. C. Lau, B. D. Hoffmann, A. Davies, J. C. Crocker, and T. C. Lubensky, Phys. Rev. Lett. **91**, 198101 (2003).
[17] S. C. Cowin, L. Mosssalentijn and M. L. Moss, J. Biomech. Engin.-Transact. of the ASME **113**, 191 (1991).
[18] F. Gittes and C. F. Schmidt, Opt. Lett. **23**, 7 (1998).
[19] M. W. Allersma, F. Gittes, M. J. deCastro *et al.*, Biophys. J. **74**, 1074 (1998).
[20] F. Gittes, and C. F. Schmidt, Method Cell Biol. **55**, 129 (1998).
[21] R. G. Bacabac, D. Mizuno, C. F. Schmidt *et al.*, J. Biomech. **41**,1590 (2008).
[22] E. Helfer, S. Harlepp, L. Bourdieu *et al.*, Phys. Rev. E **63**, 021904 (2001).
[23] T. Harada and S. I. Sasa, Phys. Rev. Lett. **95**, 130602 (2005).
[24] D. P. Kiehart, and R. Feghali, J. Cell Biol. **103**, 1517 (1986).
[25] Y. Hatwalne, S. Ramaswamy, M. Rao, and R. A. Simha, Phys. Rev. Lett. **92**, 118101 (2004).
[26] L. D. Landau and E. M. Lifshitz, *Theory of Elasticity*, 3rd ed. (Pergamon Press, Oxford, 1986).
[27] P. Bursac, B. Fabry, X. Trepat *et al.*, Biochem. Biophys. Res. Commun. **355** (2), 324 (2007).
[28] F. C. MacKintosh, and A. J. Levine, Phys. Rev. Lett. **100**, 018104 (2008).
[29] T. Yeung, P. C. Georges, L. A. Flanagan *et al.*, Cell Motil. Cytoskel. **60**, 24 (2005).
[30] A. J. Engler, S. Sen, H. L. Sweeney *et al.*, Cell **126**, 677 (2006).
[31] M. Prass, K. Jacobson, A. Mogilner *et al.*, J. Cell Biol. **174**, 767 (2006).